LOW-FREQUENCY AND ULTRA-WIDEBAND MEMS ELECTROSTATIC VIBRATION ENERGY HARVESTER POWERING AN AUTONOMOUS WIRELESS TEMPERATURE SENSOR NODE

Y. Lu [1], F. Cottone [1, 2], S. Boisseau [3], F. Marty [1], D. Galayko [4], and P. Basset [1]
[1]Université Paris-Est / ESYCOM / ESIEE Paris, Noisy-le-Grand, France
[2]University of Perugia, Dept of Physics and Geology, NIPS Laboratory, Perugia, Italy
[3]CEA, Leti, Minatec Campus, Grenoble, France
[4]UPMC-Sorbonne Université / LIP 6, CNRS, Paris, France

ABSTRACT

We report a 1-cm² ultra-wideband MEMS electrostatic vibration energy harvester (e-VEH) that combines a frequency-up conversion system with a vertical electret layer obtained by corona discharge. At 2.0 g_{rms}, the device can harvest more than 1 µW from 59 to 148 Hz, and more than 0.5 µW from 14 to 152 Hz. Thanks to this new device, we demonstrate the self-starting power supply of an energy autonomous temperature sensor node with a data transmission beyond a distance of 10 m at 868 MHz.

INTRODUCTION

It is commonly considered that the widely existing wideband low-frequency vibrations present in the environment are good sources for powering portable electronics or sensors. Vibration energy harvesters (VEHs) are typically made of a movable mass vibrating at the same frequency as the external excitation. The mechanical vibrations of this mass are then converted into electrical energy by an electro- mechanical transducer.

The mechanical power of the device is limited by the movable mass and its maximum displacement [1]. Thus, one of the bottlenecks in improving the power performance of MEMS VEHs is that their size constrains both the movable mass and its displacement [2]. Another difficulty is related to expanding the bandwidth without losing too much power at the optimal working frequency. If we develop a resonant system that offers large mechanical amplification, there is a dilemma lying intrinsically in the system: when we try to improve its power at the resonance frequency, the frequency bandwidth becomes very narrow [3-4]. If we use systems without resonant structures, the bandwidth can be very large [5-6], but these structures could hardly provide satisfying gain in the mechanical response and then, their output powers remain highly limited.

One of the most commonly used solutions is to introduce nonlinearities in the resonant system [7-9]: nonlinear devices perform well for noisy wideband vibrations, but they are less efficient for narrow-band signals. Another major solution is to realize a Frequency Increased Generator (FIG) that couples a high-frequency resonant structure with a low-frequency one through impacts [10-11]. However, the implementation of a low-frequency resonant structure makes it difficult to reduce the size of the device.

In this article, we propose an electrostatic VEH that implements a non-linear structure in a FIG-like structure. Moreover, in order to simplify the fabrication process, we also introduce the corona charging method to inject charges on vertical parylene layers to form electrets.

DEVICE DESCRIPTION

Shown in Figure 1 are a simplified schematic and a photograph of the wideband low-frequency VEH. The device is developed from a design previously reported in [9] and [12]. It is essentially a transducer with a variable capacitor consisting of interdigited gap-closing combs. The core of the device is a single-layered silicon structure. A movable proof mass is connected to two fixed ends by linear serpentine springs. On both fixed ends, there are elastic beams opposing to semi-cylindrical protrusions (or stoppers) on the movable mass. When the elastic beams are bended by the knock from the stoppers, the stiffness of the beams adds to the stiffness of the entire spring system. In the center of the movable mass, a cavity housing a tungsten-carbide miniature ball is created. Within a large range of frequencies, the ball impacts with the proof mass, and triggers its vibration at its resonance frequency. Thus, the device could extract energy from vibrations with a large bandwidth.

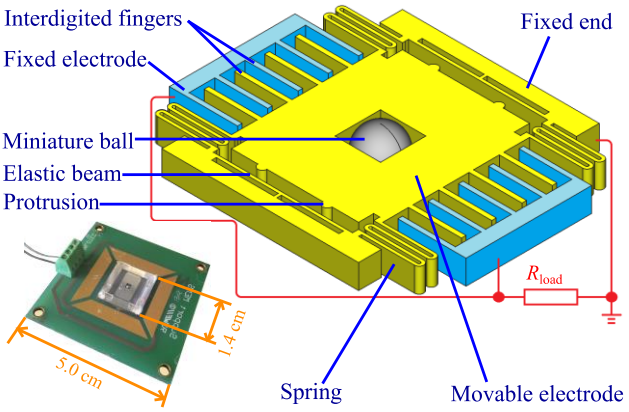

Figure 1. Simplified schematic and photograph of the prototype.

The fabrication of the device is basically a simple batch process as described in [12]. The silicon substrate is patterned by an aluminum mask on top of it, and anodically bonded with a pre-etched glass wafer. A layer of parylene-C is deposited on the full device, and the electret on the movable electrode is charged negatively by point-grid-plane corona with temperature control. The setup for the corona charging and the control of the temperature are shown in Figure 2.

In order to ensure that only the electret on the movable part is charged, the counter electrode is biased at the same voltage as the grid during the charging. The sample is

heated to 100˚C during the first 30 min, and cooled to room temperature in the following 30 min, keeping the high voltages on all the electrodes. Once the built-in voltage on the electret becomes stable, it is measured to be 33 V according to the method described in [13].

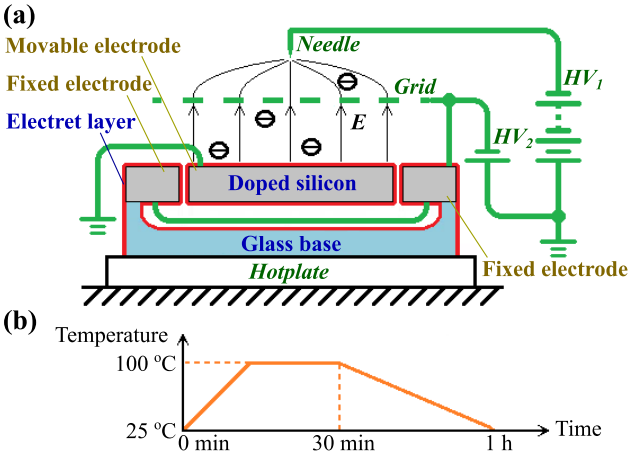

Figure 2. Corona charging of the electret layer on the movable part: (a). Experimental setup (b). Temperature control of the hotplate.

MODELING OF THE DEVICE

The device optimization has been obtained thanks to the development of a new theoretical model based on lumped parameters differential equations of a 2-DOF hybrid dynamic system. An ad-hoc numerical algorithm based on the Heun's integration method simulates the dynamic of the silicon mass-spring-damping oscillator along with the collision detection of a bouncing ball of radius *r*, which slides within a length *L* of the rectangular cavity.

Figure 3 shows the simulated harvested power (*P*) versus the normalized cavity length (*L*/2*r*). It is shown that for the case of a running man (high acceleration), an increased cavity length provides higher output power; the maximum power is reached for a normalized cavity length of 10, which is a bit too large for a small-scale device. For the walking man case, the power is maximized when the normalized cavity length is approximately equal to 2. Here, we adopt this value for the normalized cavity length (*L*/2*r*=2), leading to satisfactory performances in both cases.

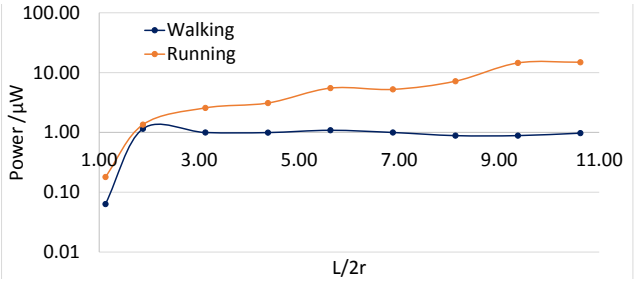

Figure 3. Simulated power versus normalized cavity length L/2r.

The mechanical-to-electrical conversion performed by the comb gap-closing capacitor is also modeled. Figure 4 shows the simulated system excited by the vibration of a running person. The RMS acceleration is about 1.3 *g*, while the peak value reaches about 9 *g*. With this acceleration, the ball travels across the cavity and impacts with the silicon proof mass. The frequency-up conversion mechanism is shown in Figure 4, where the silicon mass's displacement is compared to the micro-ball's: whenever a new peak appears in the acceleration, the ball travels across the entire cavity and bounces on its upper and lower cavity walls thus triggering the oscillation of the silicon mass. The output voltage of the transducer is correlated with the silicon mass displacement and shows peaks when the bounces takes place.

The frequency up-conversion could be clearly seen also through an FFT of the input acceleration and the output voltage (Figure 5): the major components of the acceleration are contained within the range of 2~10 Hz, while a sharp peak of the output voltage is around 17 Hz. The ultra-low frequency components of the input acceleration are all converted up in frequency, and result in a single-frequency component of output voltage. The frequency of the output voltage peak (17 Hz) is much lower than the resonance frequency of the silicon mass (104 Hz). This is due to the frequent interrupt of the oscillation of the silicon mass by the springless ball.

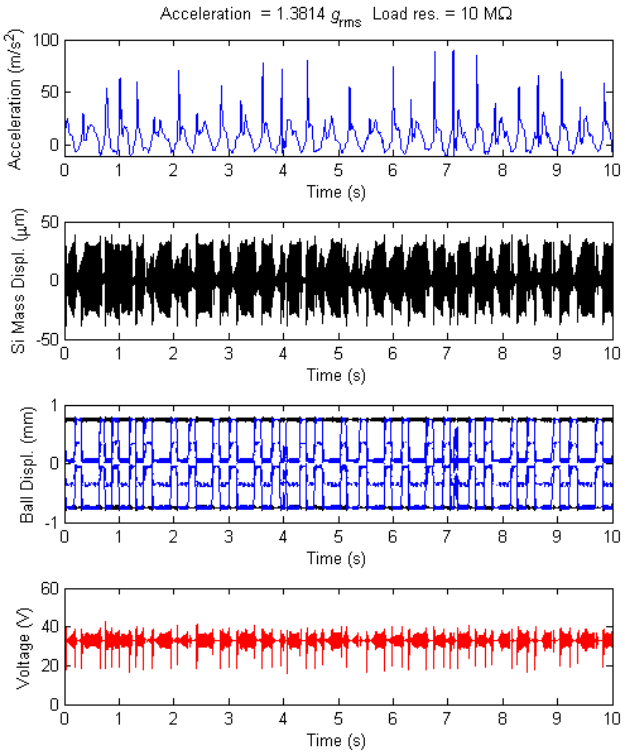

Figure 4. Simulation of the device for an acceleration corresponding to a running man.

TESTS AND DISCUSSION

The prototype is connected to a load of 10 MΩ and is subjected to power measurements with frequency sweeping. As shown in Figure 6, when working at 0.5 g_{RMS}, the output power is above 0.1 µW within 59~113 Hz. With an increased acceleration, both the power and the bandwidth are improved. At 2.0 g_{RMS} the device provides a maximum output power of 2 µW at 139 Hz, and no less than 0.5 µW within the range of 14~152 Hz.

For each acceleration, the frequency response shows chaos behavior within specific range. The chaos dynamic is governed by the alternation between triggering and interrupt of the silicon proof mass's oscillation by the impacts of the ball. And this is majorly caused by the phase difference between the ball and the silicon proof mass. With the increase of acceleration, the frequency range of chaos in voltage moves upward. In fact, at higher acceleration, less time is needed by the ball to travel across the cavity. Hence, the higher bouncing rate results in a higher effective stiffness of the system.

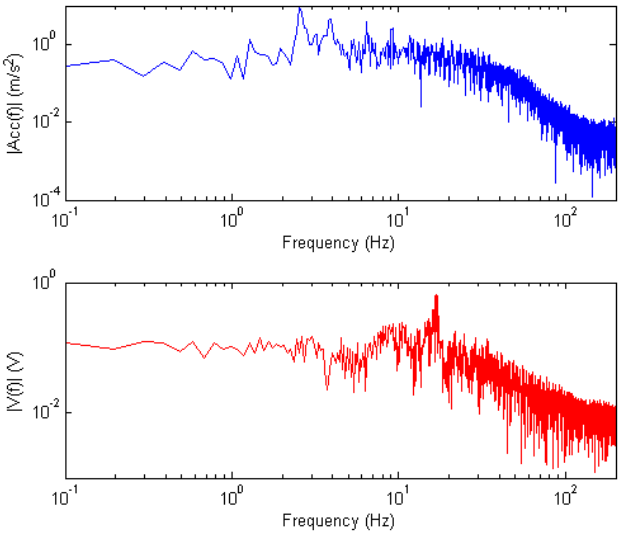

Figure 5. Spectrum of the input acceleration of a running man and corresponding output voltage given by the simulation.

It could be observed that at low frequencies with sufficient accelerations (i.e. 1 or 2 g_{rms}), the slope of the power curves is lower than 1 in the double-logarithmic chart. This indicates that the energy harvested in each period of external vibration increases with the drop of frequency. Thanks to this phenomenon, the bandwidth of the device is broadened by the miniature ball towards the low frequency range.

It is also shown that the optimal working frequency increases with the growth of acceleration. This phenomenon is majorly due to the presence of the elastic beams: with the growth of acceleration, the movable mass hits the elastic beams harder and the bending of the beams becomes larger. Thus, the effective spring stiffness of the entire system greatly increases, leading to a higher resonance frequency.

In order to reach large accelerations at low vibration frequencies, the device has also been shaken by hand, the corresponding results are marked with bolded crosses in the same *P-f* graph. At 2 g_{rms} and 5.1 Hz, the output power is 80 nW, and the average energy per cycle of external vibration is 15.6 nJ. At 1 g_{rms} and 2.5 Hz, the power is 21 nW, and the average energy per cycle of external vibration is 8.7 nJ. The power at low frequencies drops greatly compared to the frequency sweeps above 10 Hz. This drop is probably due to the damping effect of air, which stops the oscillation of the movable mass before the next knock of the ball. If a vacuum package is applied, the duration of the oscillation could be improved, and the power at low frequencies (e.g. hand-shaking) should be enhanced.

The following experiments validate a data-transmission application with the proposed energy harvester. As shown in Figure 7, an energy-autonomous Wireless Sensor Node (WSN) has been made by connecting a MEMS harvester to a low-power transmitter through a conditioning circuit. Thanks to this conditioning circuit, the energy harvested by the e-VEH is stored in a capacitor C_s = 47 µF. A self-powered Schmitt trigger reads the voltage across C_s and turns on the transmitter as soon as C_s reaches 3.5 V; it switches the transmitter off when C_s reaches 2.5 V [14].

The energy stored in C_s is used to power a data transmission of a wireless communicating sensor node. The wireless sensor node suitable for this specific application is based on a MSP 430 chip from TI, which communicates with its receiver at 868 MHz. The chip ID and the data acquired by the internal temperature sensor are sent in 0.16 s. With the proposed configuration, 102 µJ are required for a full data transmission beyond 10 m, which corresponds to a voltage drop on C_s from 3.5V to 2.8V.

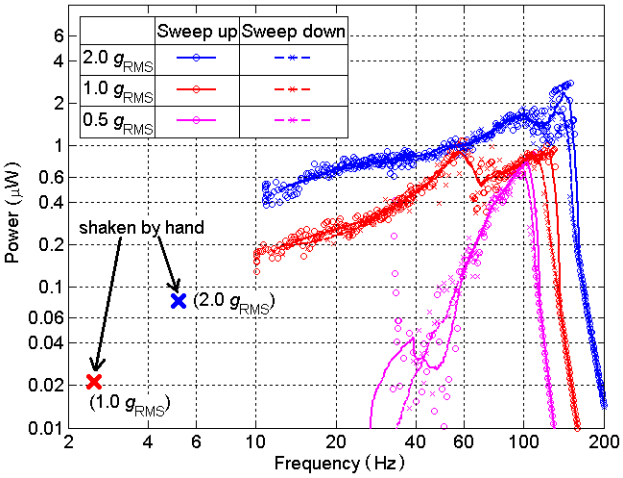

Figure 6. Average output power versus frequency at 0.5, 1 and 2 g_{rms}.

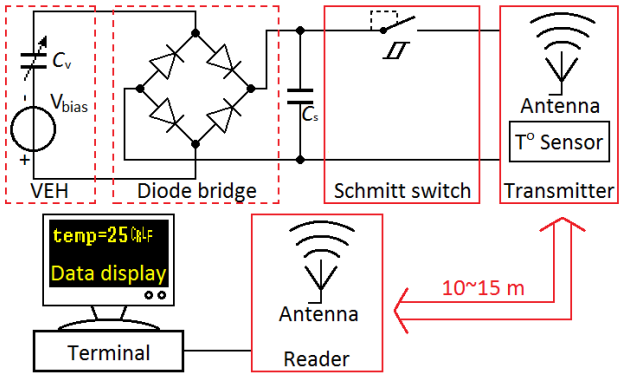

Figure 7. Schematic of the data transmission experiment.

Figure 8 shows the evolution of the voltage V_s on C_s during a charging process of a 47-µF capacitor when the e-VEH works at the frequency of 130 Hz. With 2.0 g_{RMS}, the charging takes 13.8 min for V_s to rise from 0 to 3.5 V,

while the rising from 2.5 to 3.5 V takes 4.3 min. Then, if we place the device on a 130 Hz vibrating source at 2 g_{rms}, the initial data communication occurs in 14 min and the following data transmissions take place every 4.3 min. At 1 g_{rms}, the initial data transmission takes place after 28 min of continuous vibration, and the following transmissions happen every 8 min.

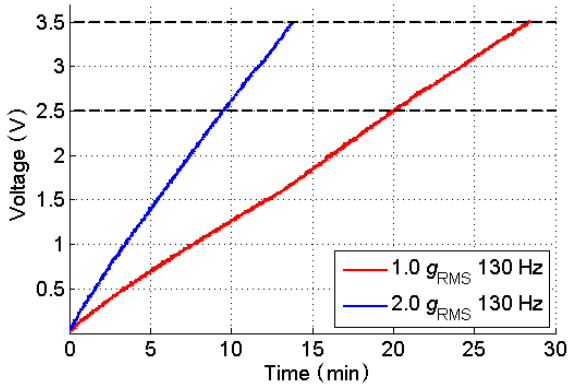

Figure 8. Charging of C_s=47 µF with the device working with an acceleration of 1.0 g_{rms} and 2.0 g_{rms} at 130 Hz.

CONCLUSION

We proposed an electrostatic wideband low-frequency VEH, with frequency up-conversion structures including a springless mass, a FIG-like structure, linear springs, and non-linear elastic stoppers. Thanks to this design, the device is capable to harvest vibration energy from a few Hz up to about 150 Hz. In addition, the electret in the device, having an in-plane electrical field, is produced by a vertical corona discharging process. In order to meet the power requirements of a wireless sensor node, the energy harvested by the VEH is stored into a capacitor through a diode bridge rectifier. Then, a Schmitt trigger controls the energy stored in C_s and releases the energy as soon as V_s = 3.5 V to supply a low-power wireless temperature sensor node. The communication node is able to send data every 4.3 min when the VEH is placed on a 2 g_{rms} @ 130 Hz vibrating source. The 868 MHz communication node could send data beyond 10 m.

Moreover, there is still a large margin of improvement to increase the output power of the energy harvester; for example by increasing the surface voltage of the parylene electret [13].

ACKNOWLEDGEMENTS

This work is partially sponsored by the SATT-IDFINNOV. The authors also thank the European Commission under FP7 Marie Curie IEF for the support of Grant agreement n. 275437.

REFERENCES

[1] P. D. Mitcheson, *et al.* Energy harvesting from human and machine motion for wireless electronic devices, *IEEE, Proceedings of*, vol. 96, pp. 1457-1486, 2008.

[2] P. D. Mitcheson, *et al.* Architectures for vibration-driven micropower generators, *Microelectromechanical Systems, Journal of*, vol. 13, pp. 429- 440, 2004.

[3] Y. Suzuki, *et al.* A MEMS electret generator with electrostatic levitation for vibration-driven energy-harvesting applications, *Micromechanics and Microengineering, Journal of*, vol. 20, 104002, 2010.

[4] J. Zhao, *et al.* Electrostatic charge sensor based on a micromachined resonator with dual micro-levers, *Applied Physics Letters*, vol. 106, 233505, 2015.

[5] H. Liu, *et al.* Piezoelectric MEMS energy harvester for low-frequency vibrations with wideband operation range and steadily increased output power, *Microelectromechanical Systems, Journal of*, vol. 20, pp. 1131-1142, 2011.

[6] Y. Lu, *et al.* A non-resonant, gravity-induced micro triboelectric harvester to collect kinetic energy from low-frequency jiggling movements of human limbs, *Micromechanics and Microengineering, Journal of*, vol. 24, 065010, 2014.

[7] D. Miki, *et al.* Large-amplitude MEMS electret generator with nonlinear spring, *Micro Electro Mechanical Systems (MEMS), Int. Conf. on*, 23rd, pp. 176-179, 2010.

[8] C. P. Le, and H. Einar. Wide tuning-range resonant-frequency control by combining electro-mechanical softening and hardening springs, *Transducers & Eurosensors XXVII, Proc. Int. Conf. on*, 17th, pp. 1352-1355, 2013.

[9] P. Basset, *et al.* Electrostatic vibration energy harvester with combined effect of electrical nonlinearities and mechanical impact, *Micromechanics and Microengineering, Journal of*, vol. 24, 035001, 2014.

[10] T. Galchev, *et al.* A piezoelectric parametric frequency increased generator for harvesting low-frequency vibrations, *Microelectromechanical Systems, Journal of*, vol. 21, pp. 1311-1320, 2012.

[11] T. Takahashi, *et al.* Vertical capacitive energy harvester positively using contact between proof mass and electret plate-Stiffness matching by spring support of plate and stiction prevention by stopper mechanism, *Micro Electro Mechanical Systems (MEMS), Int. Conf. on*, 28th, pp. 1145-1148, 2015.

[12] F. Cottone, *et al.* Electrostatic generator with free micro-ball and elastic stoppers for low-frequency vibration harvesting, *Micro Electro Mechanical Systems (MEMS), Int. Conf. on*, 27th, pp. 385-388, 2014.

[13] Y. Lu, *et al.* Low-frequency MEMS electrostatic vibration energy harvester with corona-charged vertical electrets and nonlinear stoppers, *Proc. Int. Conf. PowerMEMS* 2015.

[14] STMicroelectronics/CEA Patent pending

CONTACT

*Y. Lu, tel: +33-145-926694, Université Paris-Est / ESYCOM / ESIEE Paris, Noisy-le-Grand, France; yingxian.lu@esiee.fr